ESTIMATING EAR CANAL GEOMETRY AND EARDRUM REFLECTION COEFFICIENT FROM EAR CANAL INPUT IMPEDANCE

Huiqun Deng and Jun Yang

Institute of Acoustics, Chinese Academy of Sciences, Beijing, China 100190

ABSTRACT

Based on the signal model of ear canals, a novel method for solving the inverse problem of estimating the unique solution of the ear canal area function and the eardrum reflection coefficient given the acoustic input impedance at the entrance of an ear canal is presented. Up-sampling techniques to improve the accuracy of the estimates are also presented. The performance of this method and factors affecting the accuracy of the estimates are investigated via simulations. It is found that the accuracy of the estimates is limited by the measurement bandwidth of the given ear canal input impedance. In the audio frequency range, the estimates obtained approximate well to the true ones. To obtain more accurate estimates, a wider measurement bandwidth of the ear canal input impedance is required.

***Index Terms*—** Ear canal area function, eardrum reflection coefficient, acoustic impedance, inverse method

1. INTRODUCTION

Ear canal cross-sectional areas and eardrum reflection coefficients are important factors determining the sounds received at human ears, and their measurements are important in many applications such as middle-ear pathology, psychoacoustic measurements, hearing aid design, and sound reproduction via headphones, to mention a few. It is difficult and invasive to measure ear canal area functions and eardrum reflection coefficients inside human ear canals [1-4]. Some non-acoustical methods such as CT scan and laser measurements of the ear canals and eardrum vibrations cannot reveal the acoustic transformation properties of the ears. Therefore, the development of non-invasive acoustical methods to measure ear canal area functions and eardrum reflection coefficients has been a research topic.

Estimating ear-canal area functions and eardrum reflection coefficients from acoustic measurements at the entrances of ear canals are considered to be non-invasive. Similar inverse problems have been encountered in speech signal processing to estimate vocal-tract area functions from acoustic measurements at lips. Based on the Webster's wave equation, it is known that the spatial Fourier coefficients of a vocal-tract area function are related to the formant frequencies of the vocal tract assuming that the glottal boundary is rigid [5-6]. However, the assumption about glottal boundary is unrealistic. To exclude the reflections from unknown glottal impedance, short-time sound pressure signals at the lip opening in response to a unit impulse of volume velocity are used to derive the area functions of vocal tracts based on the Webster's wave equation [7-8]. This method has been adopted to estimate ear canal area functions and the eardrum impedances at reference planes [9]. However, direct measurements of the required short-time sound pressure impulse responses are difficult. A gradient method for estimating the ear canal area function from the phase response of the reflection coefficient of an ear canal above 3 kHz is presented [10]. This method suffers from the problems of slow convergence. In [11], the time-domain reflection coefficient at the entrance of an ear canal is obtained via inverse Fourier transform of the frequency-domain reflection coefficient of the ear canal, and is used to estimate the ear canal area function according to the Webster's wave equation. However, the solution to the eardrum reflection coefficient is not provided. A method for jointly estimating the ear-canal area function and the parameters of a simplified middle-ear impedance model is proposed via nonlinear optimization given the measured reflection coefficient of an ear canal [12]. However, the resulting estimates may be degraded by the simplified middle-ear model and initial values of the optimization.

The present work models an ear canal as a multi-sectional tube with a varying cross-sectional area function, and derives the relationship between the input impedance of the ear canal and the ear-canal area function and the eardrum reflection coefficient at the eardrum reference plane, based on the signal model of ear canals. From this relationship, the ear canal area function and the reflection coefficient at the reference plane are estimated, without imposing any model of middle ear impedances, and hence the potential degradation to the estimates caused by initial values and in-accurate assumptions about the middle ear impedance is avoided. In Sec. 2, the signal model of ear canals is presented, and the relationship between the input impedance of the ear canal and the ear canal geometry and eardrum reflection coefficient is derived. In Sec. 3, the simulations to validate the method and investigate the factors affecting the estimation accuracy are presented.

2. INVERSION METHOD

The goal of this section is to solve for the ear canal area function and the eardrum reflectance given the input impedance of the ear canal. It is known that below 15 kHz, sound waves in ear canals can be assumed as planar waves, and an ear canal can be modeled as an acoustic tube with a varying cross-sectional area function, and the effect of the eardrum can be modeled as a concentrated impedance Z_{TM} connected to the ear canal at the umbo point [13, 14]. The portion of the ear canal from its entrance to the eardrum reference plane, which is the plane of wave front at the umbo position, is modeled as an M-sectional tube with equal sectional length L, as shown in Fig. 1, where the first section starts from the entrance of the ear canal. The terminal impedance of the M^{th} section Z_T is formed by the parallel impedance of the eardrum impedance Z_{TM} and the input impedance of the residual ear canal beyond the reference plane.

Let the reflection coefficient from the end of the M^{th} section be r_T, which is determined by Z_T and the M^{th} cross-sectional area as shown in [14]. It is noted that r_T corresponds to the eardrum reflection coefficient measured at the reference plane in human ears, and contains the effect of both eardrum impedance and the residual ear canal. Let $u_m^+(t)$ and $u_m^-(t)$ be the going-in and going-out volume velocities at the beginning of the m^{th} section, respectively, m=1, …, M. Let $U_m^+(f)$ and $U_m^-(f)$ be the Fourier transforms of $u_m^+(t)$ and $u_m^-(t)$, respectively. In the frequency domain, the continuity of sound pressure and the continuity of volume velocity at the boundary of the m^{th} and $(m+1)^{th}$ sections lead to the following equation [14],

$$\begin{bmatrix} U_m^+(f) \\ U_m^-(f) \end{bmatrix} = \frac{e^{jk_m L}}{1 + r_m} \begin{bmatrix} 1 & r_m \\ r_m e^{-jk_m 2L} & e^{-jk_m 2L} \end{bmatrix} \begin{bmatrix} U_{m+1}^+(f) \\ U_{m+1}^-(f) \end{bmatrix} \tag{1}$$

where
$$k_m = 2\pi f / c - j0.0582\sqrt{f} / D_m c, \tag{2}$$

$$r_m = (S_{m+1} - S_m) / (S_{m+1} + S_m) \tag{3}$$

D_m is the diameter of the m^{th} section, c is the sound speed and S_m is the cross-sectional area of the m^{th} section. Define

$$G_m(f) \equiv U_m^-(f)/U_m^+(f) \tag{4}$$

Then, from Eqs. (1) and (4) the following equation holds:

$$G_{m+1}(f) = (r_m e^{-jk_m 2L} - G_m(\mathrm{f})) / (r_m G_m(f) - e^{-jk_m 2L}) \tag{5}$$

$G_1(f)$ is related to the input impedance of the ear canal $Z_1(f)$:

$$Z_1(f) = \frac{P_1(f)}{U_1(f)} = \frac{U_1^+(f) - U_1^-(f)}{U_1^+(f) + U_1^-(f)} \frac{\rho \mathrm{c}}{\mathrm{S}_1} = \frac{1 - G_1(f)}{1 + G_1(f)} \frac{\rho \mathrm{c}}{\mathrm{S}_1} \tag{6}$$

where $P_1(f)$ and $U_1(f)$ are the Fourier transforms of the total sound pressure and total volume velocity at the entrance of the ear canal, respectively, S_1 is the area of the entrance of the ear canal, and ρ is the air density. Eq. (6) leads to

$$G_1(f) = (1 - Z_1(f)\mathrm{S}_1/ \rho c) / (1 + Z_1(f)\mathrm{S}_1/ \rho c). \tag{7}$$

Assume that the tube attenuation can be ignored, i.e., $k_m=2\pi f/c$, that the sound signals are sampled at a rate F_s, and that the sectional length L of the tube model is related to F_s and the sound speed c as

$$F_s=c/2L. \tag{8}$$

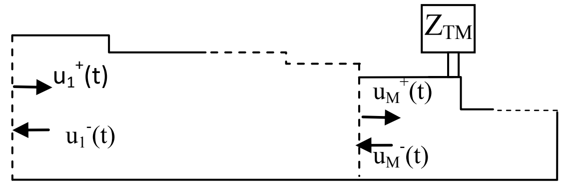

Fig. 1 The tube model of an ear canal.

Then, the discrete-time signals in the tube model (Fig.1) can be represented using their Z transforms as shown in Fig. 2 [15], where $r_T(z)$ is the Z transform of the reflection coefficient from the end of the M^{th} section. In the Z domain, Eq. (5) becomes

$$G_{m+1}(\mathrm{z}) = (r_m z^{-1} - G_m(\mathrm{z})) / (r_m G_m(\mathrm{z}) - z^{-1}) \tag{9}$$

where $G_m(z)$ is the Z transform corresponding to $G_m(f)$. According to the signal flow graph shown in Fig. 2, $G_m(z)$ is the transfer function of an IIR (Infinite Impulse Response) filter, and can be expressed as

$$\begin{aligned} G_m(z) &= r_m z^{-1} + (1 - r_m^2) r_{m+1} z^{-2} + \ldots \\ &= g_m(1) z^{-1} + g_m(2) z^{-2} + \ldots \end{aligned} \tag{10}$$

where $g_m(n)$ is the impulse response of $G_m(z)$. Eq. (10) means that

$$g_m(n)=0, \ n<=0, \tag{11}$$

and that

$$g_m(1) = r_m \tag{12}$$

Given $g_m(n)$, we derive $g_{m+1}(n)$, the impulse response of $G_{m+1}(z)$, as follows.

Inserting the second line of Eq. (10) into Eq. (9) leads to the following equation:

$$G_{m+1}(z) = \frac{(r_m - g_m(1))z^{-1} - g_m(2)z^{-2} - g_m(3)z^{-3} - \ldots}{(r_m g_m(1) - 1)z^{-1} + r_m(g_m(2)z^{-2} + g_m(3)z^{-3} + \ldots)} \tag{13}$$

Inserting Eq. (12) to Eq. (13), then $g_{m+1}(n)$ and $g_m(n)$ are related as:

$$\begin{aligned} &(g_m^2(1) - 1)g_{m+1}(n-1) + g_m(1)\,(g_m(2)g_{m+1}(n-2) + g_m(3)g_{m+1}(n-3) + \ldots) \\ &= -g_m(2)\delta(n-2) - g_m(3)\delta(n-3) - \ldots = -g_m(\mathrm{n}) \end{aligned} \tag{14}$$

Replacing n with $n+1$ in Eq. (14) leads to the following equation:

$$g_{m+1}(n) = \frac{-g_m(n+1) - g_m(1)\sum_{i=1}^{n-1} g_m(i+1) g_{m+1}(n-i)}{g_m^2(1) - 1} \tag{15}$$

Thus, for $m=1, \ldots M-1$, $g_{m+1}(n)$ can be derived from $g_m(n)$ according to Eqs. (15), r_m, can then be obtained from $g_m(1)$ according to Eq. (12), S_{m+1} can be derived from S_m according to Eq. (3), $G_{m+1}(f)$ can be derived from $G_m(f)$ according to Eq. (5). $g_1(n)$, which is the impulse response of the volume velocity reflection coefficient from the entrance

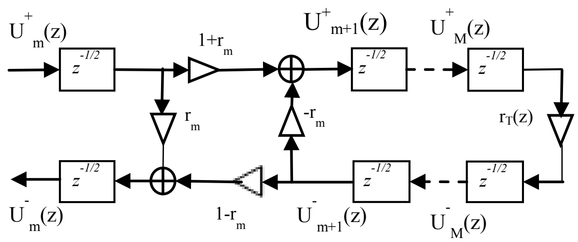

Fig. 2 The *Z*-domain signal model of the ear canal.

of the ear canal, is the key to the inverse solution. $g_1(n)$ can be obtained from the inverse Fourier transform of $G_1(f)$. $G_1(f)$ can be determined from the input impedance $Z_1(f)$ of the ear canal according to Eq. (7). $Z_1(f)$ and S_1 can be measured at the entrance of the ear canal. The performance of this method is investigated via simulation in the next section.

3. SIMULATION

3.1. Synthesis of the input impedance of the ear canal

The focus of the present paper is on the new method for obtaining the ear canal area function and the eardrum reflection coefficient at the eardrum reference plane given the input impedance of the ear canal, rather than the measurements of the ear canal impedances and area functions of human ears, which are nontrivial tasks. Therefore, synthetic input impedances of a model ear canal are used to investigate the performance of the proposed method.

The cross-sectional radius of the ear canal model in Fig.1 is determined according to the model ear canal specified in [16] at positions [0.5, 1, 1.5, …, 27] mm from the entrance of the ear canal, as shown using the thin line in the middle-right panel of Fig. 3. The sectional length of the ear canal model is L=0.5 mm. The total length of the ear canal is 27 mm, and the umbo position is at 4 mm from the end of the ear canal. The eardrum impedance Z_{TM} values at frequencies f=[5, 10, 15, …, 15000] Hz [14] are used here, and the magnitude and phase responses of Z_{TM} are plotted using the thick dotted lines in the top-left and the top-right panels of Fig.3, respectively. Given the ear canal cross-sectional area and Z_{TM}, the input impedance of the ear canal Z_1 is calculated iteratively according to [17]

$$Z_m = \frac{\rho c}{S_m}\left(Z_{m+1} + j\frac{\rho c}{S_m}\tan(k_m L)\right) / \left(\frac{\rho c}{S_m} + jZ_{m+1}\tan(k_m L)\right) \quad (16)$$

where Z_m, $m=M, M\text{-}1, \ldots, 1$ is the impedance looking from the beginning of m^{th} section into the end of the ear canal, and $Z_{M+1} = Z_T$. Z_T is calculated given Z_{TM} and the ear canal area function as shown in [14]. The magnitude and phase responses of Z_T and Z_1 are plotted using dash and solid lines, respectively, in the two top panels of Fig.3.

3.2. Inverse solution

Given Z_1 and the area of the entrance of the ear canal S_1, then the frequency response of $G_1(f)$ is calculated according to Eq. (7). The magnitude and phase responses of $G_1(f)$ are plotted using dash-dot lines in the bottom-left and bottom-right panels of Fig.3, respectively. The upper frequency limit of Z_{TM} and $G_1(f)$ is 15 kHz. If the inverse Fourier transform of $G_1(f)$ is used as $g_1(n)$, then the sampling rate for the inversion is F_s=30 kHz, and the sectional length for the inversion of the ear canal geometry is $L_{inv}=c/2F_s$=5.9 mm, which is low in the spatial resolution considering that the average length of ear canals is about 27 mm. The spatial resolution can be improved by obtaining an up-sampled $g_1(n)$ as follows.

First, according to the signal flow shown in Fig.2, one can model $G(z)$ as an IIR filter with N poles and N zeros. The optimal $G(z)$ that matches $G_1(f)$ is obtained via the Matlab function "invfreqz(h,w,n,m)", given the values of $G_1(f)$ at frequencies f=[5, 10, 15, …, 15000], the sampling rate F_{s1}=30.1 kHz, and $G(z=e^{j\pi})=G_1(f=15\text{kHz})$. In this work, the optimal N value is determined such that the maximum difference between $G_1(f)$ and $G(z=e^{j2\pi f/Fs1})$ is minimum compared to that given by other N values in the range of 30 and 130:

$$\overset{*}{N} = \underset{30<N<130}{\mathrm{argMin}}\left(\max_i \left| G_1(f_i) - G(e^{j2\pi f_i/F_{s1}}) \right|\right) \quad (17)$$

where $f_i \in f$. Second, obtain the impulse response of $G(z^\sigma)$, where σ=20, followed by a low-pass filter with a cut-off frequency 15 kHz at the sampling rate $F_{sinv}=\sigma F_{s1}$=602 kHz. Let $g_1(n)$ be sampled at F_{sinv} and truncated to length M=6000. The frequency response of $G(z^\sigma)$ at frequencies f_{inv}=[0, F_{sinv}/M, …., $(M-1)F_{sinv}/M$] is calculated. To apply the low-pass filter to $G(z^\sigma)$, set the frequency response of $G(z^\sigma)$ to zeros for $15000<f_{inv}<F_{sinv}-15000$ Hz. The inverse Fourier transform of the low-pass filtered frequency response of $G(z^\sigma)$ yields $g_1(n)$ at the sampling rate F_{sinv}, as shown in the middle-left panel of Fig. 3. The sectional length for the estimate of the ear canal area function is $L_{inv'}=c/2F_{sinv}=0.29$ *mm* in this case.

Given $g_1(n)$, then $g_m(n)$, r_m, m=2, …, is derived according to Eq. (15) and Eq. (12), respectively. Given $G_1(f)$, S_1 and r_m, then $G_m(f)$ and S_m, m=2, …, are derived according to Eq.(5) and Eq. (3), respectively. For this simulation, the first maximum negative peak of $g_1(n)$ is located at about 0.1398 ms (middle-left panel of Fig.3), which corresponds to a reflection plane at a distance L_1=24.6 mm from the entrance of the ear canal, *i.e.*, about L_2=1.6 mm beyond the eardrum reference plane. Thus, S_m and G_m can only be estimated up to $m<=(L_1-L_2)/L_{inv'}$. The radius of S_m is shown using the thick line in the middle-right panel of Fig.3. The magnitude and phase responses of G_m at different distances to the reference plane are shown using different lines in the

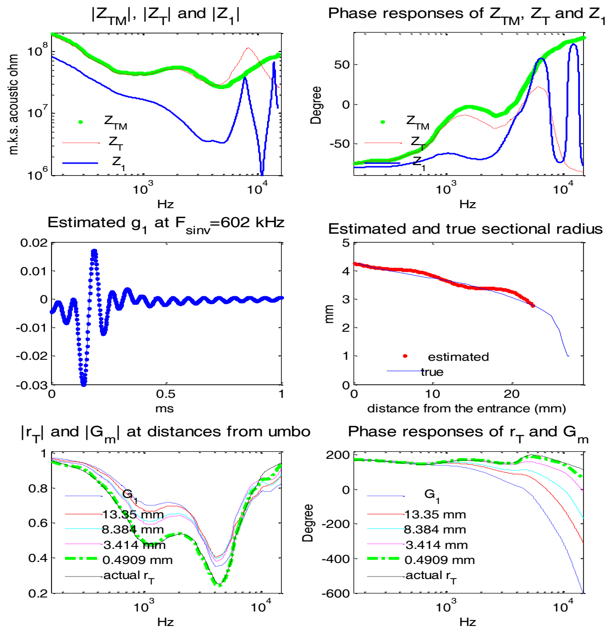

Fig. 3 Simulation given realistic ear canal impedance Z_1.

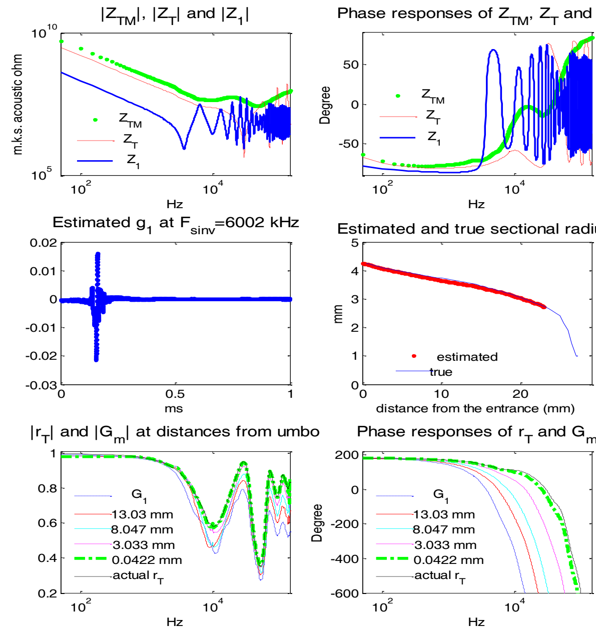

Fig. 4. Simulation given Z_1 up to 150 kHz

bottom-left and bottom-right panels of Fig. 3. In practice, the umbo position is unknown. It can be estimated that the section closest to the eardrum reference plane is numbered as $m<=(L_1-L_2)/L_{inv,}$ where L_1 can be estimated from the peak index of $g_1(n)$, and L_2 is about 1.6 mm.

3.3. Factors affecting the estimates

It is found from middle-right panel of Fig. 3 that there are some differences between the estimate of the ear canal radius function and the original one used for synthesizing Z_1, and that further up-sampling of $g_1(n)$ cannot reduce the differences. This is explained by the limitation in the bandwidth of the given input impedance Z_1. It is known that the m^{th} spatial Fourier coefficient of the area function of a tube with a varying sectional area is related to the m^{th} resonance frequency of the tube [5-6]. Since the given input impedance of the ear canal is limited to audio frequencies, only the first a few resonance frequencies of the ear canal are available, and hence only the first a few spatial Fourier coefficients of the ear canal area function can be obtained, resulting in an incomplete set of the spatial Fourier coefficients to represent the area function of the ear canal. To verify this cause, another simulation is performed assuming that the frequency response of the given Z_1 are specified at f=[50, 100, …, 150000] Hz, which is synthesized according to Eq. (16) with the values of Z_{TM} and hence Z_T being specified at f=[50, 100, …, 150000] Hz. The magnitude and phase responses of the "super-bandwidth" Z_{TM}, Z_T and Z_1 are shown in the top panels of Fig. 4 using the dotted green line, the dash red line and the solid blue line, respectively. For the cases with F_{s1}=300.1 kHz and σ= 20, the same procedure as described in Sections 3.1-3.2 is applied. It is shown in middle-right panel of Fig.4 that the estimate of the ear canal radius function is nearly equal to the true one. Similar results are obtained for σ=10, 30, 40, confirming the effect of bandwidth on the estimate of ear canal geometry.

It is noted that for both cases shown in Figs. 3 and 4, when m^{th} section does not contain the eardrum reference plane, as the distance between the beginning of the m^{th} section and the eardrum reference plane decreases, $G_m(f)$ approximates r_T more and more . In the inversion, the tube attenuation is assumed according to Eq. (2) as given in [18]. For estimation on real human ears, a realistic assumption about the tube attenuation of the ear canal is required to obtain accurate estimate of eardrum reflection coefficients. It is also found (not shown) that the estimate of the ear canal area function is not affected by assumed tube attenuation.

4. CONCLUSION

The present method shows that the unique solution of the ear canal area function and the eardrum reflection coefficient at the reference plane given the input impedance of an ear canal can be derived based on the signal model of ear canals, without using middle-ear models, and the problems of such models and non-linear optimization are avoided. The method is expected to have applications in hearing aid and headphone system design, middle ear pathology, auditory model, psycho-acoustic measurements, etc.

5. REFERENCES

[1] H. Hudde, “Estimation of the area function of human ear canals by sound pressure measurements,” J. Acoust. Soc. Am. vol. 73, no. 1, pp.24-31, Jan. 1983.

[2] M. R. Stinson, and B. W. Lawton, “Specification of the geometry of the human ear canal for the prediction of sound-pressure level distribution,” J. of Acoust. Soc. Am., *vol.***85**, no. 6, pp.2492-2503. Jun. 1989.

[3] S. E. Voss and J. B. Allen, “Measurement of acoustic impedance and reflectance in the human ear canal,” J. Acoust. Soc. Am. vol. 95, no. 1, pp. 372-384, Jan. 1994.

[4] H. Hudde, and A. Engel, “Measuring and Modeling Basic Properties of the Human Middle Ear and Ear Canal. Part I: Model Structure and Measuring Techniques,” Acustica- asta acustica Vol. 84 (1998), pp. 720-738.

[5] M. R. Schroeder, “Determination of the Geometry of the Human Vocal Tract by Acoustic Measurements” J. Acoust. Soc. Am. vol. 41, no. 4 (Part 2), pp.1002-1010, Apr. 1967.

[6] P. Memelstein, “Determination of the Vocal-Tract Shape from Measured Formant Frequencies” J. Acoust. Soc. Am. vol. 41, no. 5, pp. 1284-1294, May 1967.

[7] M. M. Sondhi and B. Gopinath, “Determination of Vocal-Tract Shape from Impulse Response at the Lips,” J. Acoust. Soc. Am. vol. 49, no. 6, pp. 1867-1873. Nov. 1970.

[8] M. M. Sondhi and J. R. Resnick, “The inverse problem for the vocal tract: Numerical methods, acoustical experiments, and speech synthesis,” J. Acoust. Soc. Am. vol. 73, no.3, pp.985-1002, Mar. 1983.

[9] M. Joswig, “Impulse response measurement of individual ear canals and impedances at the eardrum in man,” ACUSTICA Vol. 77 (1993), pp. 270-282.

[10] H. Hudde, A. Engel, and A. Lodwig, “Methods for estimating the sound pressure at the eardrum,” J. Acoust. Soc. Am. vol. 106, no. 4, pp.1977-1992, Oct. 1999.

[11] Daniel M. Rasetshwane and Stephen T. Neely, “Inverse solution of ear-canal area function from reflectance” J. Acoust. Soc. Am. vol. 130, no.6, pp. 3873-3881, Dec. 2011.

[12] J. D. Lewis and S. T. Neely, “Non-invasive estimation of middle-ear input impedance and efficiency,” J. Acoust. Soc. Am. vol. 138, no. 2, pp. 977-993, August, 2015.

[13] M. R. Stinson, and G. A. Daigle, “Comparison of an analytic horn equation approach and a boundary element method for the calculation of sound fields in the human ear canal,” J. Acoust. Soc. Am. vol. 118, no. pp. 2405-2411, Oct. 2005.

[14] H. Deng and J. Yang, “Modeling and estimating acoustic transfer functions of external ears with or without headphones,” J. Acoust. Soc. Am. vol. 138, no. 2, pp.694-707, Aug. 2015.

[15] H. Deng and J. Yang, “Simulating External-Ear Transfer Functions,” 21th International Conference on Sound and Vibrations, Beijing, China, July 2014.

[16] Hudde, H. and Engel, A. “Measuring and Modeling Basic Properties of the Human Middle Ear and Ear Canal. Part III: Eardrum Impedances, Transfer Functions and Model Calculations,” Acustica- asta acustica vol. **84** (1998), pp. 1091-1109.

[17] L. E. Kinsler, A. Frey, and J. V. Sanders, *Fundamentals of Acoustics*, 4th ed. John Wiley &Sons, inc., 2000.

[18] H. Hudde, and A. Engel, “Measuring and Modeling Basic Properties of the Human Middle Ear and Ear Canal. Part II: Ear Canal, Middle Ear Cavities, Eardrum, and Ossicles,” Acustica- asta acustica Vol. 84 (1998), pp. 894-913.